Traffic 2009; **10:** 1414–1428

doi:10.1111/j.1600-0854.2009.00968.x

Transportin Mediates Nuclear Entry of DNA in Vertebrate Systems

Aurelie Lachish-Zalait[1,†], Corine K. Lau[2,†], Boris Fichtman[2], Ella Zimmerman[1], Amnon Harel[3], Michelle R. Gaylord[2], Douglass J. Forbes[2,*] and Michael Elbaum[1,*]

[1] *Department of Materials and Interfaces, Weizmann Institute of Science, Rehovot 76100, Israel*
[2] *Section of Cell and Developmental Biology, Division of Biological Sciences, University of California-San Diego, La Jolla, California 92093*
[3] *Department of Biology, Technion - Israel Institute of Technology, Haifa 32000, Israel*
**Corresponding authors: Douglass J. Forbes, dforbes@ucsd.edu and Michael Elbaum, michael.elbaum@weizmann.ac.il*
[†] *These authors contributed equally to this work.*

Delivery of DNA to the cell nucleus is an essential step in many types of viral infection, transfection, gene transfer by the plant pathogen *Agrobacterium tumefaciens* and in strategies for gene therapy. Thus, the mechanism by which DNA crosses the nuclear pore complex (NPC) is of great interest. Using nuclei reconstituted *in vitro* in *Xenopus* egg extracts, we previously studied DNA passage through the nuclear pores using a single-molecule approach based on optical tweezers. Fluorescently labeled DNA molecules were also seen to accumulate within nuclei. Here we find that this import of DNA relies on a soluble protein receptor of the importin family. To identify this receptor, we used different pathway-specific cargoes in competition studies as well as pathway-specific dominant negative inhibitors derived from the nucleoporin Nup153. We found that inhibition of the receptor transportin suppresses DNA import. In contrast, inhibition of importin β has little effect on the nuclear accumulation of DNA. The dependence on transportin was fully confirmed in assays using permeabilized HeLa cells and a mammalian cell extract. We conclude that the nuclear import of DNA observed in these different vertebrate systems is largely mediated by the receptor transportin. We further report that histones, a known cargo of transportin, can act as an adaptor for the binding of transportin to DNA.

Key words: DNA import, gene delivery, histones, importin β, nuclear import, nuclear pores, permeabilized HeLa cells, transportin, Xenopus

Received 19 February 2008, revised and accepted for publication 21 July 2009, uncorrected manuscript published online 27 July 2009

Many viruses have developed specific strategies to promote the nuclear uptake of their genomes by the host (1,2). The addition of exogenous oligonucleotides to cells has separately been used for both viral- and non-viral-based gene therapy (3,4). In some studies, genetic transformation by the added DNA can take place on a time scale faster than cell division, implying that DNA import across the interphase nuclear envelope must occur *in vivo* (5). Indeed, a large number of studies have gone on to demonstrate that DNA entry through the nuclear pore occurs and can be enhanced by artificially coupling the DNA to peptides containing nuclear localization signals (NLSs), implying translocation across the nuclear pore (6–14).

The existence of endogenous free non-chromosomal DNA *in vivo* has also been described (15–17). Some of these studies involved cytoplasmic DNA. Interestingly, it was reported that human lymphocytes could be immortalized by fusion with enucleated cytoplasts derived from established tumor cell lines, including mouse L929 and Erlich ascites cells (18–20). The active agent responsible for immortalization was shown to be extrachromosomal cytoplasmic DNA (20). Transfecting this same DNA similarly caused immortalization. We presume that transformation of non-dividing cells could well require nuclear import of the DNA. For all these reasons, DNA entry to the nucleus deserves a close examination.

Nuclear pores are large protein complexes each comprised of ∼30 different proteins present in multiple copies, embedded in the double-membrane nuclear envelope of cells from yeast to humans. The massive nuclear pore mediates essentially all trafficking of proteins and RNAs between the nucleus and cytoplasm (21–27). The basic structure of the nuclear pore consists of an eightfold symmetric central scaffold, eight cytoplasmic filaments and a nuclear basket (28–30). Approximately one third of the nuclear pore proteins contain phenylalanine-glycine or FG repeats (31), which have been shown to interact with soluble transport receptors.

Nuclear transport receptors in large part derive from a single protein family, the importin β or karyopherin β superfamily (22,23,32–37). These receptors recognize specific NLSs or nuclear export signals (NESs) on protein or RNA cargoes, and then ferry those molecules across the nuclear pore (38). Upon entering the nucleus, interaction of the receptor with the small GTPase Ran in its GTP-bound form leads to accumulation of the cargo there ('nuclear import') or alternatively depletion from the nucleus ('nuclear export') (37,39–41).

Best known among the transport receptors is importin β, the founding member of the importin β superfamily (42–45). Importin β (or karyopherin β1), through its adaptor importin α (46), recognizes the so termed canonical or *classical* NLS, which is characterized generally as a short peptide containing basic amino acids (47–50). A second major receptor, transportin (or karyopherin β2A) binds directly to different cargoes, such as the heterogeneous nuclear ribonucleoprotein A1 (hnRNP A1). HnRNP A1 contains a 38-amino acid, glycine-rich NLS signal, specifically referred to in many studies as the M9 NLS (51,52). Recently, one study emanating from a crystal structure of the M9 peptide bound to transportin revealed a general set of rules for transportin NLSs (53). Transportin NLSs are 20–30 residues in length, have an intrinsic structural disorder and an overall basic character, with a loosely conserved N-terminal hydrophobic or basic motif and a C-terminal R-$X_{(2-5)}$ PY motif (53). Transportin mediates the import of many RNA binding and/or processing proteins, such as hnRNP A1, as well as DNA transcription factors (53). A large number of other importin β family receptors are known, but the signals that are recognized by these receptors have not been defined. However, it appears that many importin β family members carry histones into the nucleus (54,55). Notably, importin β/α has the weakest ability to transport histones, whereas transportin has the strongest (56).

Two *in vitro* systems have been widely and successfully used for 30 years to define the parameters of nuclear protein transport. In one, mammalian cultured cells are treated with digitonin to permeabilize their plasma membranes, while leaving their nuclear membranes intact (57). In a second, nuclei reconstituted *in vitro* in *Xenopus* egg extracts have provided a highly valuable system for studying both nuclear assembly and nucleocytoplasmic transport (58–61).

In previous work using reconstituted nuclei, we visually followed the nuclear uptake of DNA at the single-molecule level using optical tweezers (9). We found that individual molecules of long bacteriophage DNA attached to a latex bead were gradually and continuously drawn into the nucleus, in a manner that could be precisely measured and the conditions for nuclear uptake tested (9). DNA entry was gradual, consistent with a picture of serpentine passage through the nuclear pore. We found no evidence for involvement of an ATPase motor in moving the DNA through the pore channel, as has been characterized, e.g., in the mechanism of DNA packaging by bacteriophage ϕ 29 capsids (62) and in the DNA translocation machinery in *Bacillus subtilis* (63). The proteomic analyses of isolated nuclear pores from yeast and mammals revealed no ATPases or motors in the core nuclear pore complex (NPC) structure (29,30,64). However, the DEAD-box helicase DBP5, a known ATPase, is found strongly associated with the cytoplasmic filaments of the nuclear pores and is required for mRNA export (65,66).

In the present work, we have sought to analyze the role of nucleocytoplasmic transport receptors in DNA entry into the nucleus. Using sets of specific inhibitors and competitors, we have found that transportin mediates DNA import in *Xenopus* reconstituted nuclei. In addition, transportin also mediates nuclear entry of DNA in a well-characterized mammalian permeabilized cell assay. Moreover, biochemical analysis reveals that histones can act as a strong adaptor protein for transportin recognition of DNA.

Results

A modified Xenopus egg extract promotes transport-competent nuclei with long-term stability

Nuclei formed *in vitro* using *Xenopus* egg extract allow one to focus on DNA interactions with the nuclear pore at the nuclear envelope surface. In this *in vitro* environment, molecular access of DNA to the nuclear envelope is relatively direct. In addition, the extract provides a complete set of soluble constituents needed to support nucleocytoplasmic trafficking (9,40,58,59,67–69), nuclear and nuclear pore assembly (70–76), and mitotic spindle assembly (77–80).

As a model system for analyzing the nuclear import of DNA substrates, we first tested a classical high-speed fractionated *Xenopus* egg extract. In this protocol, a crude, low-speed extract of *Xenopus* eggs is further separated into a membrane fraction and a fraction containing soluble cytosolic components. These fractions are then combined with demembranated sperm chromatin to form nuclei (59). We observed, however, that these nuclei were often surrounded by a hazy cloud of membranes. While the cloud was difficult to observe without differential interference contrast imaging, and protein transport assays were not apparently affected, the associated membranes tended to trap the larger DNA substrates and hindered their access to the nuclear pores and envelope. Surprisingly, unfractionated crude extracts produced far less of this membranous barrier surrounding the nuclei. This led us to develop a modified protocol for a clarified crude (CCr) extract, which yielded a consistent, efficient nuclear assembly even after fourfold dilution into extract buffer (40). Moreover, protein accumulation into such nuclei was robust to the prolonged incubation required for DNA import. The nuclear envelope and nuclear pores of CCr nuclei were examined in detail, using high-resolution field-emission scanning electron microscopy (FESEM). This analysis revealed well-developed nuclei with continuous membranes bearing large numbers of nuclear pores (Figure 1) that were essentially identical to the nuclear envelopes formed in classically fractionated extracts (59).

DNA accumulates in reconstituted nuclei

To examine and compare the DNA import capability of the reconstituted nuclei, a set of fluorescently labeled

transport substrates was used. These included: (i) human nucleoplasmin fused to green fluorescent protein (GFP-NP), as a marker for the classical NLS-importin α/β-mediated pathway, (ii) the hnRNP A1, as a marker for the transportin-mediated pathway (GFP-A1) and (iii) a 1500-bp fragment of double-stranded DNA covalently labeled with Cy3 dye by which to visualize DNA entry into the nucleus. Nuclei to which these substrates were added were monitored by confocal fluorescence microscopy. A representative experiment showing efficient nuclear protein accumulation with either 10 μg/mL GFP-NP protein or 10 μg/mL GFP-A1 protein is shown in Figure 2A,B (green panels), respectively. When 20 μg/mL Cy3-DNA was added simultaneously with GFP-NP, the DNA was readily imported (Figure 2A, red). Both a nuclear rim stain and distinct punctate intranuclear foci of Cy3-DNA were observed. Thus, we conclude that fluorescent DNA import occurred in the *in vitro* system. However, when GFP-A1 and Cy3-DNA were added together, Cy3-DNA import was largely inhibited (Figure 2B, red). The degree of inhibition was sensitive to the concentration of GFP-A1 added, i.e. at concentrations of GFP-A1 lower than specified above; Cy3-DNA import was blocked less efficiently (data not shown). Together, these data suggested that DNA import can occur in the *in vitro* system but that hnRNP A1 might compete as a cargo for the same machinery.

Global import inhibitors block DNA import

Experiments on nucleocytoplasmic transport *in vitro* have employed a number of pathway-specific inhibitors. Importantly, these inhibitors have been shown to have identical effects *in vivo* (81–84). One such inhibitor is wheat germ agglutinin (WGA), a lectin that binds to the *N*-acetylglucosamine residues found on glycosylated nucleoporins and which has been found to block receptor-mediated transport through the nuclear pores (57,67,68,85). When WGA was added here, we found that WGA blocked entirely the nuclear uptake of Cy3-DNA cargo, similar to its complete inhibition of GFP-NP entry (data not shown).

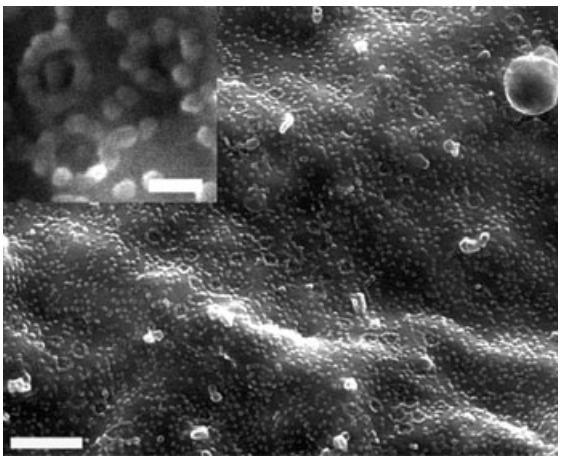

Figure 1: Scanning electron micrograph of a nucleus reconstituted in clarified crude egg extract. Numerous nuclear pores are observed at high magnification. Bars: 500 nm (large image) and 100 nm (inset).

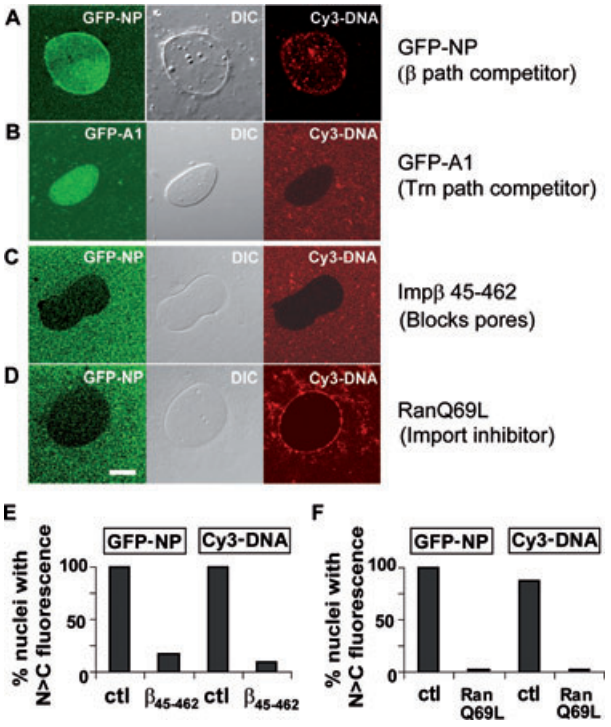

Figure 2: DNA is imported into reconstituted nuclei, but is blocked by the global inhibitors importin β 45-462 and RanQ69L-GTP. Each row presents scanning confocal images of a representative nucleus in GFP, DIC and Cy3 color channels. A) Simultaneous accumulation of GFP-NP and Cy3-DNA is observed. B) Nuclear accumulation of DNA is not observed in the presence of GFP-hnRNP A1. C) Importin β 45-462 (FG-binding domain), which is a global inhibitor of all nuclear transport, inhibits GFP-NP and Cy3-DNA accumulation. D) RanQ69L-GTP blocks nuclear uptake of both nucleoplasmin and DNA. E and F) Bar graphs of replicate experiments for (C, D). The vertical axis denotes the relative percentage of nuclei scored positive for cargo accumulation. For assays involving soluble protein substrates, 'positive' accumulation was scored if the nuclear concentration was higher than the cytoplasmic concentration. 'Non-accumulation' was scored if equal or lower concentrations were found in the nucleus. DNA import was scored as positive for cases of either higher average nuclear intensity versus background or for the appearance of intense nuclear DNA foci. Inhibitors and mock inhibition by addition of buffer (ctl) are listed on the horizontal axis. Nuclei were detected first by Hoechst staining and then checked for transport cargo to avoid biased data collection. The total number of nuclei counted for each treatment varied between 12 and 46. p-values obtained by Fisher's exact test between ctl and β_{45-462} in (E) were $p = 0.000012$ for GFP-NP and $p < 10^{-6}$ for Cy3-DNA. p-values between ctl and RanQ69L in (F) were $p = 0.0002$ for GFP-NP and $p = 0.000002$ for Cy3-DNA, thus all the p-values are significant. Bar: 10 μm.

Another established dominant negative inhibitor of nucleocytoplasmic transport is a truncated form of importin β, termed here Imp β 45-462, which contains amino acids 45-462. Imp β 45-462 binds irreversibly to FG nucleoporins (Nups) in the pore (86). Indeed, when added to nuclei Imp β 45-462 has been seen by atomic force microscopy to create a physical plug, or mound, at the central channel region of the pore through such FG-Nup binding (87). Here, when Imp β 45-462 was added to reconstituted nuclei prior to the addition of GFP-NP and DNA substrates, the nuclei were seen to exclude GFP-NP, indicating successful inhibition of transport (Figure 2C, GFP-NP). The import of DNA was also strongly inhibited by Imp β 45-462, which prevented even the binding of DNA to pores at the nuclear rim (Figure 2C, Cy3-DNA). These results are quantitated in Figure 2E.

Importin β family transport receptors are regulated in their action by the small GTPase Ran (23). Indeed, interrupting the GTP-GDP cycle of Ran is an effective means for inhibiting receptor-mediated nuclear transport. Thus, RanQ69L, a mutant of Ran incapable of hydrolyzing GTP, blocks transport by irreversibly binding to and sequestering the receptors (88). We asked whether RanQ69L-GTP blocks DNA import into nuclei. If so, this would be a strong indication for the involvement of a Ran-regulated, receptor-mediated pathway for DNA import. RanQ69L-GTP was added to assembled, reconstituted nuclei and fluorescent transport substrates were introduced 15 min later. The inhibitory competence of RanQ69L-GTP was verified by the block of GFP-NP accumulation in the nuclei (Figure 2D, GFP-NP). Similarly, Cy3-DNA was also excluded from nuclei after RanQ69L addition. Cy3-DNA decorated the nuclear envelope with a rim of adsorbed DNA molecules, but no intranuclear DNA was observed (Figure 2D, Cy3-DNA), indicating that DNA import could well employ a Ran-regulated transport receptor. The inhibition of DNA import by RanQ69L-GTP is quantitated in Figure 2F. We concluded that the Cy3-DNA import is sensitive to global inhibitors of protein nucleocytoplasmic transport, indicating the involvement of protein receptors in the nuclear import of DNA.

Inhibition of transportin leads to a block in DNA import

To further test the hypothesis that nuclear import of exogenous DNA is mediated by a protein receptor, we performed import assays in the presence of soluble inhibitors to the importin β- and transportin-mediated pathways of protein nucleocytoplasmic transport. These inhibitors are based on fragments of Nup153, a vertebrate nucleoporin located in the nuclear pore basket that serves as a major binding site for several importin family receptors (89–92). Different domains of Nup153 act as binding sites for distinct transport receptors (93). A fragment of *Xenopus* Nup153 encompassing nine FG repeats binds the importin α/β heterodimer. When bound to this fragment, importin α/β can still bind its NLS cargo, but cannot bind to FG-repeat Nups within the pore. This Nup153-FG fragment thus sequesters importin α/β and their cargoes. In this way, Nup153-FG has been shown to act as a dominant negative competitive inhibitor to classical NLS nuclear import when added to permeabilized cell assays (93). A more amino terminal fragment of *Xenopus* Nup153 deficient in FG repeats, termed Nup153-N′, has been shown to bind transportin and, in doing so, sequesters transportin away from the nuclear pores (93). The FG and N′ fragments of Nup153 therefore function as pathway-specific dominant negative inhibitors of protein transport by the importin α/β- and transportin-mediated pathways, respectively (93). This pathway-specific inhibition was confirmed here, as a control, in the permeabilized HeLa cell assay where it was originally described (Figure 5C).

The effects of the Nup153 inhibitory fragments in the *Xenopus* system were tested and we determined the optimal concentrations needed to inhibit specifically either the importin β (Nup153-FG) or the transportin (Nup153-N′) protein transport pathways (data not shown). These same optimal concentrations, 40 μM Nup153-FG and 30 μM Nup153-N′, were then assessed for an effect on DNA import into *Xenopus* reconstituted nuclei (Figure 3A–C,F,G). Specifically, nuclei were reconstituted, then Nup153-FG and Nup153-N′ at the optimized concentrations were added and the reconstituted nuclei were allowed to incubate for 20 min. At this time, the transport substrates were introduced, and accumulation in the nuclei was assessed after 20 min. As expected, Nup153-FG significantly reduced the percentage of nuclei accumulating the importin β cargo GFP-NP (Figure 3A,F, GFP-NP). It did not reduce the percentage of nuclei accumulating the transportin cargo GFP-A1 (Figure 3F). In contrast, Nup153-N′ blocked the accumulation of GFP-A1 (Figure 3B,G, GFP-A1), but not that of GFP-NP (Figure 3C,G, GFP-NP).

When Cy3-DNA was added to nuclei in the presence of the Nup153-FG β-inhibitor, fluorescent DNA foci were observed in nuclei (Figure 3A, red). Nuclear DNA foci and rim association, observed here and in Figure 2A, is a hallmark of DNA import in mammalian cells [see (7) and references therein as well as Figures 4 and 5 below]. The data for replicate experiments are graphed in Figure 3F. In contrast, when the transportin inhibitor Nup153-N′ was added, no fluorescent DNA foci were observed in the nuclei (Figure 3B,C, red). GFP-nucleoplasmin accumulation was not impacted in the same nucleus (Figure 3B, green), while GFP-hnRNP A1 uptake was blocked (Figure 3C, green). The data for replicate experiments with Nup153-N′ are graphed in Figure 3G.

Rim binding to nuclear pores has been recognized as an interim step in protein transport and is known to be dependent on the specific receptor involved (57,68,94). When Nup153-FG was added, Cy3-DNA molecules, in

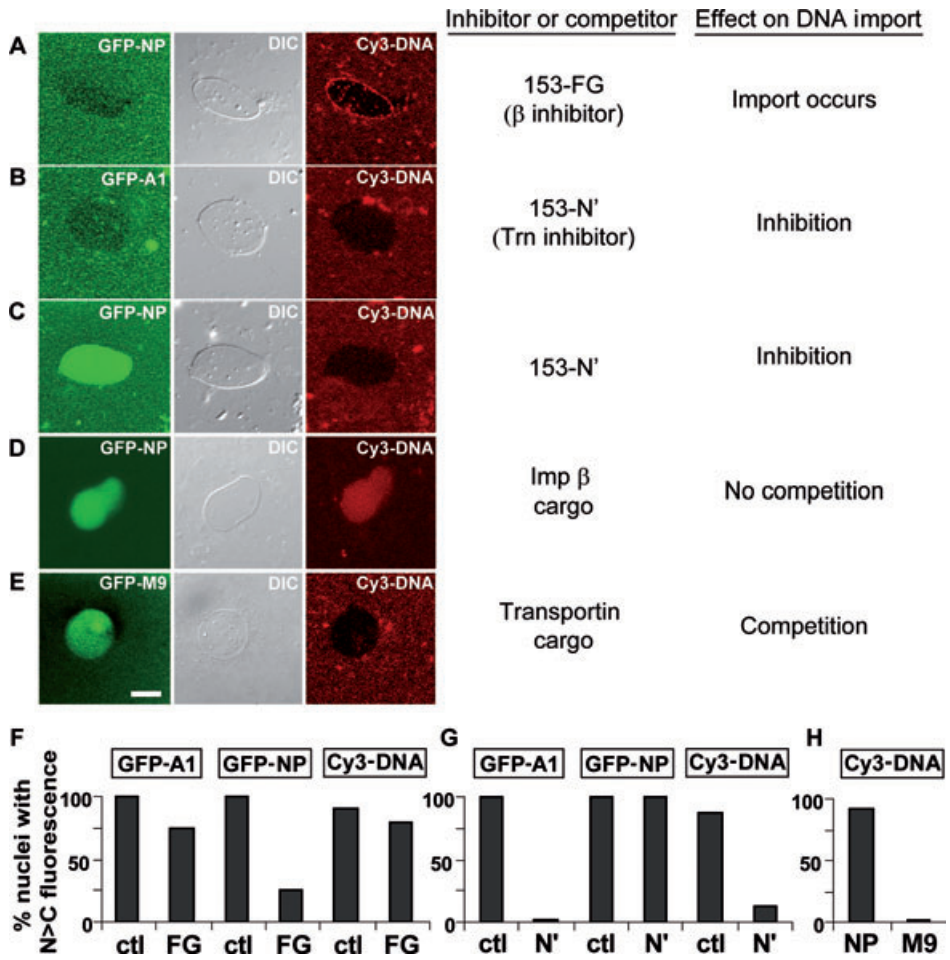

Figure 3: Multiple inhibitors of the transportin-mediated import pathway block DNA import. Each row shows scanning confocal images of a representative nucleus in GFP, DIC and Cy3 color channels. A) The importin β pathway inhibitor Nup153-FG effectively blocked the entry of nucleoplasmin. However, DNA uptake took place under these conditions, as observed from the punctate intranuclear foci that are typical of DNA import. B) The transportin pathway inhibitor Nup153-N′ inhibited both GFP-A1 accumulation and DNA uptake. C) Nup153-N′ fragment again inhibited DNA import, while nucleoplasmin accumulated in the nucleus. D) DNA and nucleoplasmin, an importin β cargo, accumulated simultaneously in the nucleus, indicating a lack of competition between these substrates for transport factors. E) GFP-M9, a transportin cargo, competed effectively with DNA, preventing its nuclear import. F–H) Replicate measurements were scored and statistical tests performed as shown in Figure 2E,F. p-values between ctl and Nup153-FG in (F) were $p = 0.33$ for GFP-A1, $p = 0.000147$ for GFP-NP and $p = 0.37$ for Cy3-DNA import. This indicates significant inhibition by Nup153-FG of GFP-NP only. p-values between ctl and Nup153-N′ in (G) were $p = 0.008$ for GFP-A1, $p = 1.000$ for GFP-NP and $p = 0.002$ for Cy3-DNA import. This confirms significant inhibition by Nup153-N′ of GFP-A1 and Cy3-DNA, but not of GFP-NP. For (H), $p = 0.000003$, confirming the suppression of DNA import by GFP-M9. Bar: 10 μm.

addition to being observed inside the nucleus, were also observed bound to the nuclear envelope, indicating that the binding step in Cy3-DNA import occurs in the presence of importin β inhibition. However, when Nup153-N′ was added, there was no Cy3-DNA fluorescence at the nuclear rim (Figure 3B,C), consistent with a lack of DNA import upon transportin inhibition. Quantification is shown in Figure 3F,G. Taken together, these data strongly implicate transportin as a receptor for the entry of DNA into the nucleus.

To further test the involvement of transportin in DNA import, we also performed a formal cargo competition assay. Even when a large excess of the importin β cargo GFP-NP (40 μM) was added, it was found to have no effect on Cy3-DNA import (Figure 3D,H). With respect to transportin, hnRNP A1 is an excellent cargo for import assays (Figure 2B) but is not ideal for competition, as it becomes insoluble at the high molar concentrations needed for completely effective competition assays. We therefore used a GFP-M9 fusion protein, which contains the M9 NLS region of hnRNP A1. GFP-M9 has been used as a transportin cargo in many studies, and is soluble at very high concentrations. In control experiments, a high excess of GFP-M9 (40 μM) was observed not to affect the importin β-mediated import of SV40-NLS-HSA, but to

block the transportin-mediated import of MBP-M3, an M9-containing fusion protein (Figure S1). Importantly, 40 μM GFP-M9 completely blocked the import of Cy3-DNA into *in vitro* assembled nuclei (Figure 3E,H). We conclude from these multiple pathway-specific inhibitors that transportin is a significant receptor for DNA import into the nucleus in this *Xenopus* system.

DNA import in permeabilized HeLa cells shows a similar dependence on the transportin pathway

To further test this conclusion, we performed DNA import analysis using permeabilized HeLa cells. Notably, these cells have previously been shown to be competent for both protein and DNA import into the nucleus (6,7,57,95,96). The permeabilized HeLa cell assay has been widely used to characterize the mechanism of nucleocytoplasmic protein transport (57,97–101). Conditions for DNA import in HeLa cells included: (i) a shorter DNA substrate (400 bp), as a longer fragment often did not enter the nucleus in a reasonable period of time, (ii) rabbit reticulocyte lysate as a source of cytosol, (iii) lower concentrations of the inhibitors to suit the more dilute reticulocyte lysate cytosol and (iv) a higher temperature (37°C) to mimic mammalian cellular conditions.

When rhodamine-labeled double-stranded 400 bp DNA fragments were added to permeabilized HeLa cells and incubated for 90 min at 37°C, distinct DNA foci were observed in the nuclei (Figure 4A, control). Consistent with translocation taking place through the nuclear pores, no nuclear DNA foci were observed if the reaction was carried out in the absence of an ATP regenerating system or in the absence of cytosolic factors (Figure S2A,B), or when the inhibitor WGA was present (data not shown). It should be noted that under both import-competent and import-inhibited conditions, DNA was also seen in the cytoplasm; this has been previously observed (3,102) and is thought to be DNA entrapped by endoplasmic reticulum (ER) and cytoskeletal barriers. We next evaluated DNA import by quantitating the number of fluorescent nuclear DNA foci observed in the presence or absence of specific transport pathway inhibitors.

When a substrate competition assay was carried out in permeabilized HeLa cells with an importin β cargo, we found that excess GFP-NP did not significantly affect the number of observed nuclear DNA foci (Figure 4A, GFP-NP, 3 and 8 μM). In contrast, when a competition assay was carried out with a transportin cargo, we found that excess GFP-hnRNP A1 completely abolished DNA import into HeLa cell nuclei; no nuclear DNA foci were observed (Figure 4A, GFP-A1, 3 and 8 μM). Quantitation is shown in Figure 4B. These results strongly reinforce the conclusion reached in the *Xenopus* experiments that DNA enters the nucleus via a transportin-mediated pathway.

To assess DNA import in the presence of pathway-specific inhibitors, Nup153-FG was added at a concentration sufficient to inhibit importin β-mediated protein transport

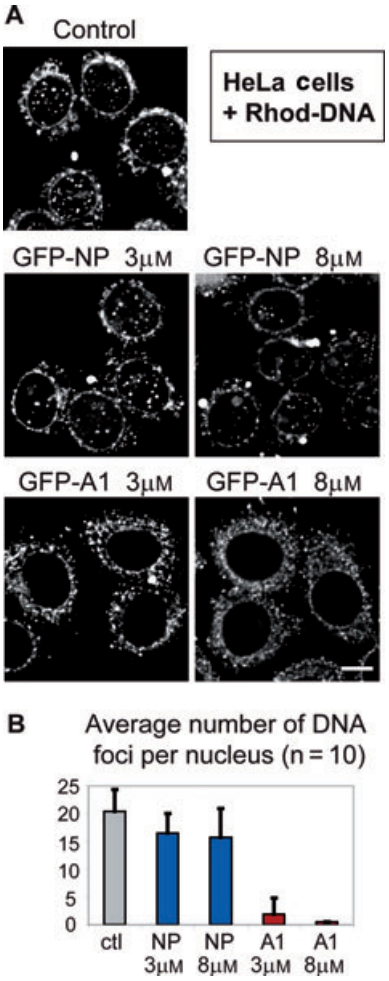

Figure 4: Excess transportin cargo, but not importin β cargo, blocks DNA import in permeabilized HeLa cells. CX-Rhodamine-labeled DNA fragments of 400 bp were added to permeabilized HeLa cells in transport mixture, with or without competing protein substrates. Cells were incubated at 37°C for 90 min and fixed for confocal microscopy. A) DNA imported into the nucleus was observed as distinct nuclear foci (control). DNA import was observed in the presence of excess of the importin α/β substrate, GFP-NP (GFP-NP, 3 or 8 μM), but not when excess GFP-A1, a transportin substrate, was present (GFP-A1, 3 or 8 μM). All images shown were projected from five z-sections at 0.5 μm spacing through the middle of the nuclei. Images were prepared using ImageJ software (http://rsb.info.nih.gov/ij/). B) The number of nuclear DNA foci in 12 nuclei per condition was counted, the highest and lowest numbers were dropped, and the average and standard deviation were plotted. Bar: 10 μm.

(2 μM). No effect was seen on DNA import into HeLa nuclei (Figure 5A, 153-FG, 2 μM), although some inhibition of DNA import was observed at higher concentrations of Nup153-FG (Figure 5A, 153-FG, 8 μM). However, addition of Nup153-N', the dominant negative transportin inhibitor, reduced DNA import dramatically at all tested concentrations (Figure 5A, 153-N', 2 and 8 μM). Quantitation of these results is shown in Figure 5B.

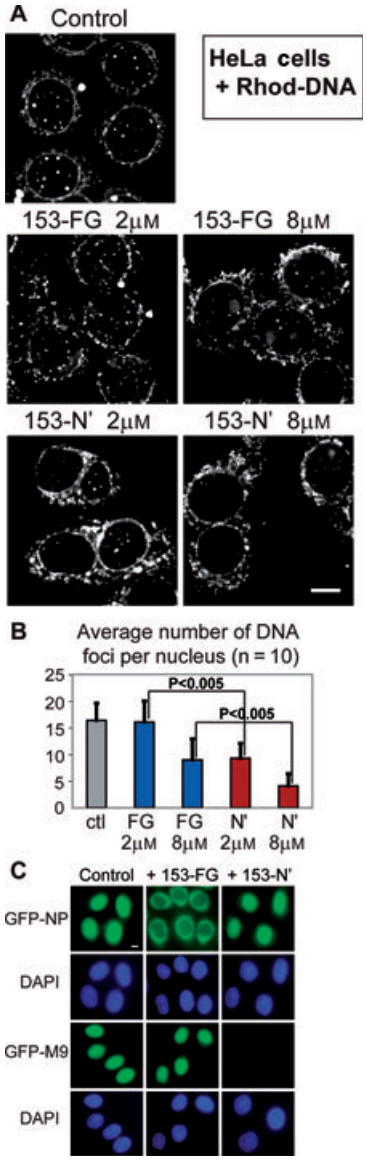

Figure 5: A dominant negative inhibitor of the transportin pathway blocks DNA import in permeabilized HeLa cells. Permeabilized HeLa cell assays were performed and images were processed as in Figure 4. A) In the presence of the importin β inhibitor Nup153-FG, a decrease in distinct nuclear foci of DNA was observed, but only at high concentration of inhibitor (153-FG, 8 μM). In the presence of the transportin inhibitor Nup153-N', DNA import was suppressed at both high and low concentrations (153-N', 2 and 8 μM). B) The number of nuclear DNA foci was counted for each inhibitor. The average number of punctate nuclear foci per nucleus and the standard deviation are shown, as in Figure 4. p-values comparing DNA foci for 153-FG and 153-N' inhibitors at the same concentrations (2 and 8 μM, respectively) were $p < 0.005$, indicating a significant difference in their effectiveness. C) To confirm specificity of the inhibition in this assay, Nup153-FG or Nup153-N' was added at a final concentration of 25 μM, while GFP-NP or GFP-M9 was present at a final concentration of 3 or 4 μM, respectively. Images shown are single planes through the *z*-axis. Bar: 10 μm.

Thus, DNA import is negatively impacted when the transportin pathway is compromised in permeabilized HeLa cells, just as it is in *Xenopus* reconstituted nuclei.

Histones serve as an adaptor between transportin and DNA

As transportin has no known DNA-binding domain, adaptors that bear both a DNA-binding motif and a transportin-recognizable NLS domain might mediate transportin-facilitated nuclear import of DNA. Histones are DNA-binding proteins where the N-terminal domains of each core histone as well as globular portions of the H2A, H2B, H3 and H4 histones can serve as NLSs (56,103). Despite their small size, core histones do not enter the nucleus by diffusion. The nuclear import of core histones has been found to be mediated by at least five nuclear transport receptors, specifically Imp β, transportin, Imp5, Imp7 and Imp9 (55). This study also showed that Imp β and Imp7 bind with relatively low affinity to all four core histones, Imp9 binds with high affinity to H2B, Imp5 binds with high affinity to H2B, H3 and H4, while transportin binds with high affinity to H2A, H2B and H3. This suggests that Imp5 and transportin might be the most potent transport receptors for core histones. Of its three histone cargoes, transportin binds H2A with the highest affinity and in a RanGTP-dependent manner. Strikingly, when Imp α and Imp β were tested in a permeabilized cell assay together, they were unable to import any of the four core histones (104), suggesting that *in vivo* Imp β may play a minor role in the import of histones. Interestingly, in agreement with Muhlhausser et al. (55), transportin showed the highest capacity amongst the import receptors tested to import core histones into the nucleus (104). Taking these studies together, we hypothesized that core histones might be good candidates for adaptors between transportin and DNA for DNA import.

First, the effect of exogenous DNA was tested on histone entry into reconstituted *Xenopus* nuclei. Recombinant human histone H2A was labeled with fluorescein and added to *Xenopus* nuclei in the presence or absence of 1500 bp linear Cy3-DNA. In the absence of exogenous DNA, H2A (14 kDa) equilibrated between the nucleus and cytoplasm or appeared slightly excluded from the nucleus (Figure 6A). However, in the presence of 1500 bp Cy3-DNA, histone H2A clearly accumulated to a higher extent in the nuclei along with the Cy3-DNA (Figure 6B). We conclude that the nuclear accumulation of histone H2A can be enhanced by the addition of exogenous DNA.

We next set out to test whether transportin binds to DNA in extract. For this, we incubated DNA-cellulose beads or unmodified cellulose beads with high-speed *Xenopus* egg extract in the presence or absence of increasing concentrations of RanQ69L-GTP. As shown in Figure 7A, transportin bound to DNA cellulose (top panel, lane 1), but was increasingly removed in a RanGTP-dependent manner (top panel, lanes 2–4). This showed that transportin indeed can bind to DNA in the presence of *Xenopus* extract, the

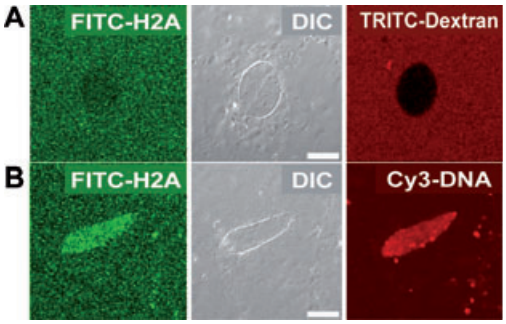

Figure 6: Nuclear accumulation of histone H2A increases when exogenous DNA is imported. Fluorescein-histone H2A was added to reconstituted *Xenopus* nuclei in the absence or presence of 1500 bp Cy3-DNA. In the absence of exogenous DNA, H2A gave a diffusion-like or weak exclusion pattern (A), while in the presence of 1500 bp DNA, histone H2A clearly accumulated in nuclei (B) along with Cy3-DNA. Bars: 10 μm.

same system which when used above (Figures 2 and 3) showed that transportin can mediate DNA import.

Knowing that transportin binds and imports histones *in vivo*, and that histones bind DNA, we tested whether histones might act as an adaptor for the binding of transportin to DNA using only purified proteins. To prevent random aggregation of histones with DNA and to facilitate interaction between core histones and DNA, recombinant NAP1, a histone chaperone, was preincubated with core histones, followed by the addition of DNA (105). Even if Nap1 was present, without added histones, transportin did not bind DNA (Figure 7B, top panel, lane 1). In the presence of added histones, GST-transportin bound plasmid DNA (pEGFP-C2) (Figure 7B, top panel, lane 2). This interaction was RanGTP sensitive, as increasing concentrations of RanQ69L-GTP disrupted DNA binding to transportin (Figure 7B, top panel, lanes 3–6). Thus, taken together with the previously published data on histone import (55,56,104), our results strongly suggest that core histones can act as adaptors between DNA and transportin during the process of transportin-mediated delivery of DNA from cytoplasm to nucleus.

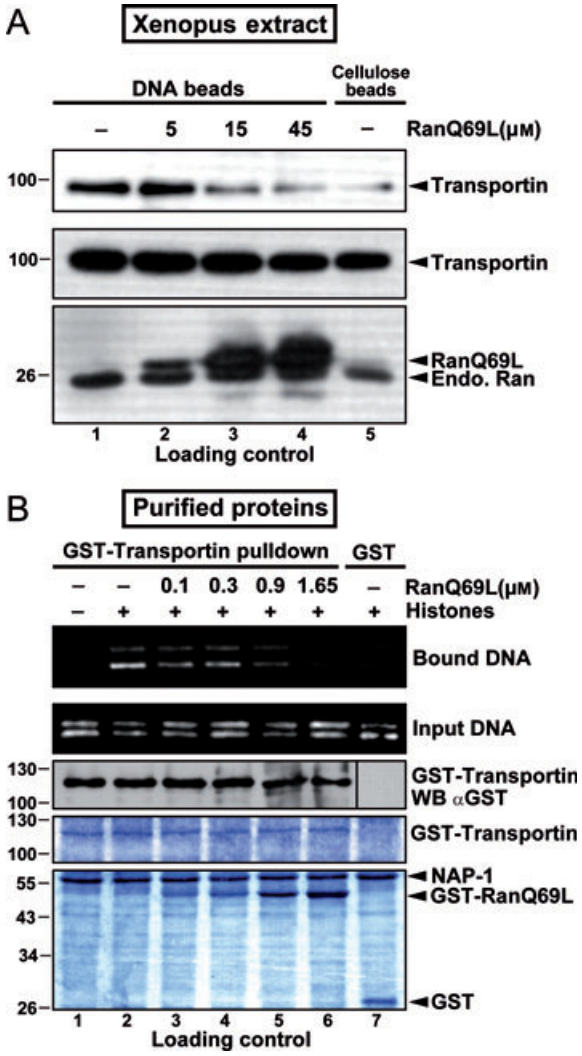

Figure 7: Core histones mediate interaction between transportin and DNA *in vitro*. A) *Xenopus laevis* transportin interacts with DNA-conjugated cellulose beads and is removed by RanQ69L-GTP. High-speed *Xenopus laevis* extract was preincubated with or without recombinant RanQ69L-GTP for 15 min on ice before the addition of DNA-conjugated cellulose beads and incubation at 4°C for 2 h. After extensive washing, the DNA beads were treated with DNase, and the bound proteins were eluted and processed for immunoblotting with anti-transportin or anti-Ran antibodies. In the top panel, lane 1 shows the amount of transportin bound to DNA cellulose in the absence of RanQ69L-GTP. Lanes 2–4 show the amount of transportin bound in the presence of the increasing concentrations of RanQ69L-GTP, and lane 5 shows the amount of transportin bound to cellulose beads lacking DNA. The bottom two panels are loading controls that show that equal amounts of transportin and endogenous Ran were present in each reaction, as determined by immunoblotting. B) *Drosophila melanogaster* core histones mediate the interaction of transportin with DNA in a Ran-reversible manner. Recombinant GST-transportin was incubated with or without RanQ69L-GTP for 15 min on ice, before the addition of a mixture containing core histones, the histone chaperone NAP1 and circular pEGFP-C2 plasmid DNA. Glutathione beads were then added and the reaction incubated overnight at 4°C, followed by six washes. The bound DNA was recovered (as described in *Materials and Methods*), separated on an agarose gel, and stained with Syber-green. For use as a loading control, 20% of the full reaction was removed before addition of the glutathione beads; half of this was treated with protease K to use for the DNA loading control (second panel; stained with Syber-green), while the other half was treated with DNAse to use for the protein loading controls. The proteins were separated on 10% SDS–PAGE and visualized with anti-GST immunoblotting (panel 3) or Coomassie blue (lower two panels).

Discussion

DNA entry into the nucleus occurs in a number of cellular processes, including certain viral infections, exogenous gene transfection and gene therapy. Viral DNA can be delivered to the pore by its capsid or can associate with viral-specific proteins that carry NLSs recognized by host cell transport receptors (1,96,106). Certainly, the latter finding validates the concept of receptor-mediated nuclear entry of DNA. In a specific example, a recent study found that transportin recognizes adenoviral protein VII on the viral DNA and through this binding mediates nuclear import of the DNA (107). In gene therapy-directed studies, when DNA was engineered to contain artificially cross-linked NLSs or NLS-bearing proteins, it showed an enhanced nuclear translocation efficiency (6–13). However, exogenous unmodified DNA that lacks artificially cross-linked NLSs can also enter nuclei, even in non-dividing cells. While the efficiency is low, this DNA entry implies that there exists a cellular mechanism for DNA import across the intact nuclear envelope (108). In most experimental models, it would be difficult to learn the rules of DNA interaction with the nuclear pore given the abundant cytoplasmic barriers that can hinder free passage of such large macromolecules to the nuclear pore (109). The cell-free *Xenopus* nuclear reconstitution system that we have used here permitted a specific focus on DNA passage through the nuclear pores, i.e. DNA substrate could be introduced without having to cross a plasma membrane or encounter the obstacles of ER or cytoskeletal structures. Our protocol for nuclear reconstitution based on partially clarified, crude *Xenopus* extract maximized this advantage.

Here we have asked whether translocation of non-viral DNA into the nucleus involves a receptor used in established pathways of nucleocytoplasmic protein transport. General inhibitors of protein transport were tested first. WGA, truncated importin β and the hydrolysis defective mutant RanQ69L all blocked nuclear entry of DNA.

When receptor-specific cargoes were used as potential competitors for DNA uptake, excess transportin cargoes GFP-hnRNP A1 and GFP-M9 (which contains the isolated NLS of hnRNP A1) strongly inhibited the nuclear uptake of DNA (Figures 2B and 3E). Furthermore, the transportin-specific dominant negative inhibitor, Nup153-N′, blocked nuclear uptake of DNA, while the importin β inhibitor Nup153-FG did not. Thus, these studies using *Xenopus* reconstituted nuclei implicated transportin as a significant receptor in the nuclear import of DNA.

Moving into mammalian cells, we attempted RNAi knockdown of transportin before transfection with fluorescent DNA. However, even very long and repeated RNAi treatments achieved only a partial reduction in transportin levels. Moreover, given the extensive list of cargo proteins normally carried by transportin (53) and thus the likelihood of interrupting multiple cellular processes, we rejected this *in vivo* approach as the cells were unlikely to survive both a long RNAi treatment to remove transportin, followed by transfection with DNA to monitor DNA import. Instead, we turned to the well-established mammalian permeabilized cell protein import assay (6,57) to examine DNA import. Nuclear protein transport has been extensively studied using this permeabilized mammalian cell system and the *Xenopus* system. When fluorescent DNA was added to permeabilized HeLa cells in this study, a fraction of DNA was always observed in the cytoplasm (Figure 4), presumably delayed on membrane and cytoskeletal components as described in a previous study using microinjection (102). Importantly, we observed the appearance of punctate DNA foci inside the permeabilized cell nuclei by 90 min. Again, this DNA accumulation was strongly inhibited by excess GFP-hnRNP A1 but not by GFP-nucleoplasmin (Figure 4). This lack of a competitive effect of importin β cargo was observed previously in permeabilized mammalian cells in a study which did not address transportin (6). Similarly to the reconstituted nuclei, we found that DNA import in the permeabilized cells was blocked by high concentrations of the transportin inhibitor Nup153-N′, but only weakly affected by the importin β inhibitor Nup153-FG (Figure 5A,B). The fact that the *Xenopus* egg extract is of embryonic origin, while the permeabilized cells are supplemented with a somatic cell extract, suggests a generality to the common observations. The results from both transport systems are clear: when the receptor transportin is blocked, DNA import falls to negligible amounts.

The known roles of transportin *in vivo* include the nuclear import of many RNA processing proteins, but also the import of DNA-binding proteins such as histones and a subset of transcription factors (53,55,110–112). Histones contain NLSs and bind DNA both *in vivo* and *in vitro*. The nuclear transport of histones has been shown to be mediated by a variety of receptors (54–56,113–116), one of the most potent of which, at least in higher eukaryotes, is transportin (55,56,104). We reasoned that histones were thus good candidates for a DNA-transportin adaptor. We found here that the addition of exogenous DNA significantly increased the accumulation of fluorescein isothiocyanate (FITC)-H2A histone into reconstituted *Xenopus* nuclei (Figure 6). This suggested a coupling between the nuclear uptake of the two substrates. We further found that transportin binds to DNA-cellulose beads that have been incubated in *Xenopus* egg extract, and that addition of recombinant RanGTP suppresses this interaction. To test a possible bridging of transportin to DNA via histones, we used purified core histones, the histone chaperone NAP1 and plasmid DNA. We found that transportin indeed binds to DNA in the presence of core histones and NAP1. In addition, the observed *in vitro* interaction between transportin, histones and plasmid DNA is disrupted by increasing concentrations of RanGTP. NAP1 itself is not an adaptor, as transportin plus NAP1 but without histones showed no binding of transportin to DNA. Taken together, our data indicate that histones

can indeed mediate the interaction between transportin and DNA, and argue further that this interaction could facilitate the transportin-mediated import of DNA that we observe. We cannot formally rule out that other DNA-binding adaptors might also be used to recruit transportin to DNA. However, the core histones are such an abundant cargo for transportin (55,56) that they may likely suffice as the major type of adaptor.

Might other import receptors also play a role in DNA import? It will only be possible to determine this once NLSs and inhibitors are identified that are *specific* for each of those receptors. However, it must be emphasized that because we find that inhibition of the transportin pathway so strongly impaired DNA import, it would appear that transportin is the most prominent in DNA import.

As mentioned earlier, a recent study found that transportin binds to adenoviral terminal protein VII and mediates the import of adenoviral DNA (107). Our finding that non-viral DNA reaches the nucleus via transportin suggests perhaps that adenovirus co-opted and then optimized an existing cellular pathway. This would further argue that the receptor transportin can be considered a potential target for modulation in both viral infection and non-viral gene delivery.

Transport of nucleic acids through the nuclear pore is well known: e.g. mRNAs, tRNAs, snRNAs and snRNPs are all transported through the pore. Clearly, one wishes to know in what circumstances DNA import occurs *in vivo*. DNA transfection occurs from yeast to humans, as we know from the laboratory. It may also be common *in vivo* as necrosis and injury likely lead to a source of extracellular DNA for transfection and potential import.

Also relevant to the overall discussion, natural instances of non-chromosomal DNA circles and fragments have been reported in a wide variety of systems (117). In yeast, ERCs (extrachromosomal ribosomal circular DNAs) are produced by homologous recombination between adjacent rDNA genes. Such circles accumulate in the nucleus as the mother cell ages (118). In this case, however, the ERCs are not released into the cytoplasm, as yeast has a closed mitosis, and thus the ERCs would not be a substrate for DNA import. In multidrug-resistant mammalian cells, the *MDR1*, *MDR2* and *EGFR* genes are often amplified to also give rise to extrachromosomal circular copies, which then recombine with one another to become the larger circular DNAs referred to as 'double-minutes' (119,120). These double-minute circles are, however, tethered in some manner to the chromosomes and do not for the most part exist as cytoplasmic DNAs (121). Multiple other organisms have also been found to have extrachromosomal DNAs, which have been implicated in genomic plasticity (122). Intriguingly, however, cases of *cytoplasmic* DNAs have also been found in mouse L929 cell lines and Erlich ascites tumor cells. These DNAs, when added to non-proliferating B cells, immortalized the B cells (18–20). Presumably, this immortalization would require DNA import because the non-proliferating B cells would not undergo mitotic nuclear breakdown. Interestingly, the transfer of mitochondrial and chloroplast DNA to the nuclear genome over evolutionary time might also have occurred through DNA import (123–125).

In summary, we have shown that DNA entry into vertebrate cell nuclei is mediated by transportin and that histones can serve as an adaptor for the binding of transportin to DNA. Our results, together with the above non-chromosomal DNA studies, show that there is rich future ground for a closer look at natural DNA entry into the nucleus.

Materials and Methods

Xenopus laevis clarified crude egg extract

Gray-amber crude extract (unfractionated cytosol and membranes) of *Xenopus laevis* eggs was prepared as in (59). It was then transferred to 2 mL tubes for a clarifying spin (34 000× g or 20 000 rpm, 15 min, 4°C) in a TLS-55 rotor (Beckman Optima TL UltraCentrifuge). CCr extract was collected by puncturing tubes just above the black pigment layer and collecting the upper solution. Sucrose (2 M) was added to a final concentration of 0.2 M as a cryoprotectant. Aliquots were frozen in liquid N_2 and stored at −80°C.

In vitro reconstitution of nuclei from clarified crude extract

Nuclei were assembled in CCr extract that had been diluted three- to fourfold with extract buffer (HEPES-NaOH pH 7.4 10 mM; KCl 50 mM; $MgCl_2$ 2.5 mM; sucrose 250 mM; BSA 20 mg/mL) and supplemented with an ATP regenerating system (final concentrations: ATP 1 mM; phosphocreatine 10 mM; creatine phosphokinase 50 μg/mL) by addition of 2000 units/μL demembranated sperm chromatin prepared as in (126). Experiments were performed immediately after nuclear assembly. However, we noted that the reconstituted nuclei could be held at 4°C for up to 24 h and still retain nuclear transport activity when restored to room temperature. Thus, these nuclei formed in CCr extract are unusually robust.

Transport assays in reconstituted nuclei

Fully assembled nuclei were supplemented with an ATP regenerating system (as above) and with the relevant inhibitor or, alternatively, with buffer as a control. WGA was added at 1 mg/mL, importin β 45-462 at 10 μM, RanQ69L at 20 μM, Nup153-FG at 40 μM and Nup153-N′ at 30 μM. Following a 20–30 min incubation, fluorescent substrates were added: GFP-NP (10 μg/mL) or GFP-hnRNP A1 (10 μg/mL) as markers for classical NLS or M9 NLS-mediated accumulation, respectively, and 1500 bp Cy3-DNA (20 μg/mL) as the DNA import substrate. In cases where only one substrate was tested, fluorescently labeled dextran [tetramethylrhodamine isothiocyanate (TRITC) or FITC-dextran, Sigma-Aldrich] was added as an exclusion marker for intact nuclei. For cargo competition assays, 40 μM GFP-M9 or GFP-NP was used. Following a 20–30 min incubation at 20°C, samples were fixed and chromatin was stained with an ultraviolet (UV)-excited DNA dye (Hoechst 33258; 2 μg/mL in 5 mM HEPES, pH 7.4; 50 mM sucrose; 2.5% paraformaldehyde) to assist in initial visual identification of the nuclei by epifluorescence. This eliminated a possible bias in scoring of transport-inhibited nuclei that otherwise might not have been identified in the transport assay itself.

Two-channel images were recorded on an Olympus Fluoview confocal microscope with PlanApo 60×/1.4 oil immersion objective. GFP is excited

at 488 nm and Cy3 at 568 nm in this microscope, ensuring a good separation of the emission channels. All results were confirmed using unfixed specimens.

Transport substrates

For assays using *Xenopus* egg extracts, fluorescent DNA was prepared from 1500-bp fragments replicated by polymerase chain reaction (PCR) from a pEGFP plasmid (Enhanced Green Fluorescent Protein; BD Biosciences Clontech), using the primers: 5′-CTCTAGAATTCCAACTGAGCG-3′ and 5′-GAACGAAAACTCACGTTAAGGG-3′. Fragments were then purified and covalently labeled with Cy3 Label IT reagent (Mirus Bio Corporation) at 37°C for 3 h. Covalent labeling avoided leakage of dye to chromosomal DNA. Excess dye was removed by purifying DNA over size exclusion mini-spin columns (Mirus Bio Corporation). The final concentration of labeled DNA was 0.1 mg/mL.

Fluorescent DNA used in the permeabilized HeLa cell assay was generated as a PCR fragment of 400 bp using EGFP primers 5′-CCCGAGCTCATGGTGAGCAAGGGCGA GGAG-3′ and 5′-CAGCTCGATGCGGTTCACC-3′ and pEGFP-N2 (BD Biosciences Clontech) as template. The PCR fragment was purified using QIAquick Gel Extraction Kit (Qiagen). Five micrograms of DNA was labeled using CX-Rhodamine Label IT Tracker Kit (Mirus Bio Corporation), according to manufacturer's instructions.

6xHis-tagged recombinant GFP-NP and GFP-hnRNP A1 (plasmid obtained from M. Michael, Harvard University) were expressed in BL21 cells (0.5 mM isopropyl-beta-D-thiogalactopyranoside (IPTG), 3 h in a shaking incubator, 36°C) and purified by fast protein liquid chromatography (FPLC) over Ni^{2+}-nitrilotriacetic acid (NTA) resin columns in native conditions (binding buffer: 20 mM Tris, pH 8, 500 mM NaCl, 20 mM imidazole; elution buffer: 20 mM Tris, pH 8, 500 mM NaCl, 400 mM imidazole). FPLC was operated in gradient elution mode and both proteins were eluted at 150–200 mM imidazole. Buffer was exchanged to PBS (8 g/L NaCl, 0.2 g/L KCl, 0.14 g/L Na_2HPO_4, 0.24 g/L KH_2PO_4) by dialysis in SnakeSkin dialysis bags (Pierce/Thermo Fisher Scientific Inc), glycerol was added to 5%, and aliquots were frozen in liquid N_2. Alternately, 6xHis-tagged GFP-NP and GFP-A1 were expressed in BL21 cells with 0.1 mM IPTG at 16°C overnight, and purified using Ni^{2+}-NTA resin columns with the same binding buffer and elution buffer (20 mM Tris, pH 8, 500 mM NaCl, 1 M imidazole). Proteins were dialyzed in PBS + 5% glycerol, and aliquots were frozen in liquid N_2.

Fluorescently labeled histone H2A

Histone H2A (Roche) (0.5 mg/mL in 0.1 M sodium carbonate buffer, pH 9) was mixed with 5 mL of a 4 mg/mL FITC (Sigma-Aldrich) in DMSO at a low dye-protein molar ratio of 2:1. After overnight incubation at 4°C, the reaction was stopped by addition of NH_4Cl to 50 mM. Excess free dye was removed by dialysis against PBS.

Transport inhibitors

Importin β 45-462, which contains the FG nucleoporin-binding domain, but lacks the RanGTP and importin α binding domains of importin β (86), was expressed and purified as described in (73). RanQ69L in pET28A was expressed, purified and loaded with GTP essentially as described in (86).

6xHis-tagged recombinant Nup153-FG and Nup153-N′ (93) were expressed in BL21 cells and purified over Ni^{2+}-NTA resin columns under denaturing conditions (binding buffer: 20 mM Tris, pH 8, 500 mM NaCl, 6 M guanidinium, 20 mM imidazole; washing buffer: 20 mM Tris, pH 8, 500 mM NaCl, 6 M urea, 20 mM imidazole; elution buffer: 20 mM Tris, pH 8, 500 mM NaCl, 6 M urea, 400 mM imidazole). FPLC was operated in gradient elution mode and both proteins were eluted at 150–200 mM imidazole. Buffer was exchanged to PBS by dialysis in 10 kDa MW cutoff SnakeSkin dialysis bags (Pierce/Thermo Fisher Scientific Inc), glycerol was added to 5% and aliquots were frozen in liquid N_2. Alternatively, 6xHis-tagged Nup153-FG and Nup153-N′ were expressed in BL21 cells with 0.1 mM IPTG at 16°C overnight, and purified using Ni^{2+}-NTA resin columns with binding buffer (20 mM Tris, pH 8, 500 mM NaCl, 20 mM imidazole) and elution buffer (20 mM Tris, pH 8, 500 mM NaCl, 1 M imidazole). Proteins were dialyzed in PBS + 5% glycerol, and aliquots were frozen in liquid N_2.

6xHis-tagged GFP-M9 was cloned from the GFP-hnRNP A1 plasmid as follows: the *GFP-hnRNP A1* gene was sequenced and primers were designed to fit the end of GFP and beginning of M9 sequences, with an insertion coding for TEV cleavage site in the middle (CTATACAAAGAATTCCACGAAAACCTGTATTTTCAGGGAG-GATATAACGA CTTTGGC and GCCAAAGTCGTTATATCCTCCCTGAAAAT-ACAGGTTTTCGT GGAATTCTTTGTATAG). A major part of the *hnRNP A1* gene (927 bp) was then deleted by deletion mutation amplification with Pfu Turbo DNA polymerase (Stratagene), leaving the C-terminal M9 region linked to 6xHis-tagged GFP through a TEV cleavage site. The parental plasmid was digested by DpnI restriction enzyme (Stratagene) leaving the truncated plasmids to be transformed into XL1B cells. Deletion mutation was verified by sequencing. GFP-M9 protein was expressed in BL21 cells. Purification was performed by FPLC over Ni^{2+}-NTA resin columns in native conditions, as described above.

Permeabilized HeLa cell transport assay

Untreated rabbit reticulocyte lysate (Promega) was used as a source of cytosolic proteins. Lysate was dialyzed versus transport buffer [20 mM HEPES, pH 7.3, 110 mM potassium acetate, 5 mM sodium acetate, 2 mM magnesium acetate, 1 mM EGTA, 2 mM DTT, 1 mg/mL aprotinin, 1 mg/mL leupeptin and 0.1 mM phenylmethylsulphonyl fluoride (PMSF)] and stored in aliquots at −80°C. Permeabilized HeLa cell import assay was performed similarly to (57). HeLa cells were grown on coverslips, rinsed once with cold PBS then cold transport buffer, permeabilized with 40 μg/mL digitonin (high purity grade, Calbiochem/EMD Chemicals Inc) in transport buffer for 3–5 min on ice, followed by two rinses in transport buffer. Four microliters of rabbit reticulocyte lysate, 1 μL energy regenerating system (1 mM ATP, 5 mM phosphocreatine and 75 μg/mL creatine phosphokinase), 0.5 μL CX-Rhodamine-labeled DNA, and/or fluorescent protein substrates (GFP-NP or GFP-A1 or GFP-M9; final concentration at 3 or 8 or 4 μM, respectively) and/or transport receptor inhibitors (Nup153-FG or Nup153-N′; final concentration at 2 or 8 μM) were mixed and added to coverslips in a 40 μL reaction and incubated at 37°C for 90 min. The samples were then rinsed in transport buffer, fixed in 4% formaldehyde for 10 min at 23°C, rinsed 2× in PBS, and mounted on microscope slides with Vectashield (Vector Laboratories) with 4′-6-Diamidino-2-phenylindole (DAPI) for confocal microscopy.

Permeabilized HeLa cells were visualized with an Axiovert 200M microscope (Carl Zeiss) at a magnification of 40× using an oil objective (Carl Zeiss) with a 1.3 numerical aperture. Images were recorded using a Coolsnap HQ (Photometrics) camera and Metavue software (Molecular Devices Corporation).

Field-emission scanning electron microscopy

Samples were prepared essentially as described in (127). Fully assembled nuclei (4–10 μL) were adhered onto 5 × 5 mm^2 silicon chips by gently suspending in 1 mL extract buffer, and then spinning them down onto the chips in a swinging bucket rotor at 1000 × ***g*** for 10 min at 4°C. Silicon chips with adherent nuclei were then transferred into fix buffer (80 mM PIPES-KOH, pH 6.8; 1 mM $MgCl_2$; 150 mM sucrose; 2% paraformaldehyde; 0.25% glutaraldehyde) for 10 min at room temperature, followed by two gentle washes in 0.2 M cacodylate and postfixation in 0.2 M cacodylate with 1% OsO_4. Samples were stained with 1% uranyl acetate, dehydrated in ethanol, and critical point dried from ultra-dry CO_2 (BAL-TEC CPD 030), sputter coated with 3.4 nm chromium (EMITECH K575X), and examined using a field emission scanning electron microscope (FEI, XL30 ESEM FEG).

Statistical tests

Transport assays using reconstituted nuclei were scored in a binary fashion. For assays involving soluble protein substrates, 'positive' accumulation was scored if the nuclear concentration was higher than the cytoplasmic, whereas equal or lower concentrations were scored as non-accumulating. DNA import was scored positive both in cases of higher average nuclear intensity versus background, and for the appearance of intense nuclear foci. For the data in Figures 2 and 3, characterized by binary choice, statistical significance was determined using Fisher's exact test with one-tailed probability (http://www.danielsoper.com/statcalc/calc29.aspx). For the data in Figures 4 and 5 where a continuum of values for the number of DNA foci within nuclei was possible, the Student's *t*-test available from Microsoft Excel software was used.

DNA-cellulose bead pulldown of transportin

To determine whether transportin present in the *Xenopus* extract can bind directly or indirectly to DNA, DNA-conjugated cellulose beads were used. DNA-cellulose beads (Sigma-Aldrich, D8515) and microgranular cellulose (Sigma-Aldrich, C6413) were blocked with 50 mg/mL BSA in egg lysis buffer with sucrose (ELBS) (HEPES 10 mM pH 7.8; KCl 50 mM; $MgCl_2$ 2.5 mM; sucrose 250 mM). High-speed *Xenopus* extract was pre-cleared with blocked microgranular cellulose for 1 h at 4°C. Pre-cleared *Xenopus* extract (28 μL) was supplemented with either buffer (ELBS) or increasing concentrations of RanQ69-LGTP (2 μL total supplement) for 15 min on ice. The reaction (30 μL) was diluted with 250 μL ELBS+ (ELBS; EDTA 0.2 mM; DTT 1 mM; Triton-X-100 0.01%; protease inhibitors), mixed with 5 μL (bed volume) of beads and incubated for 2 h at 4°C. The beads were washed 3× with ELBS+, twice with ELBS, followed by treatment with DNAse (100 μg/mL in PBS; DTT 10 mM; Triton-X-100 1%; $MgCl_2$ 10 mM) for 30 min on ice. Proteins were eluted with 5× Laemmli sample buffer, subjected to gel electrophoresis and immunoblotting with anti-transportin and anti-Ran (BD Transduction Laboratories) antibodies.

GST-transportin pulldown of DNA

To determine whether transportin could bind directly to DNA or could bind indirectly to DNA in the presence of histones, a glutathione S-transferase (GST)-transportin pulldown was used. Glutathione beads were blocked with 20 mg/mL BSA and 20 mM dNTPs for 1 h at 4°C. First, *Drosophila melanogaster* recombinant NAP1 (4.5 μg) plus (lanes 2–7) or minus (lane 1) purified *D. melanogaster* core histones (1.5 μg) in 20 μL of ELBS + 0.1% BSA were incubated for 20 min at room temperature. Then, 0.5 μg of circular plasmid DNA (pEGFP-C2) was added. At this time, a mix of GST-hTransportin (5 μg) and increasing concentrations of RanQ69L-GTP (0–16.5 μg) in 20 μL ELBS + 0.1% BSA (preincubated for 15 min on ice) was added to each of the tubes above. Immediately 20% of each reaction was taken, 10% for the DNA loading control and 10% for protein loading controls. ELBS (163 μL) and blocked glutathione beads (5 μL) were then added to each reaction, giving a final concentration of 0.2 μM transportin and 0.1, 0.3, 0.9, 1.65 μM RanQ69L-GTP, before incubation overnight at 4°C with shaking. Beads were washed with washing buffer (ELBS + 0.1% BSA + 0.01% Tween) 3×. Next, three washes were performed with increasing concentrations of KCl (100, 150 and 200 mM) in washing buffer. After each wash, the beads were collected by gravity on ice. For the experimental test (top panel) proteins bound to the beads were removed by digestion with protease K, before extraction of the DNA with phenol/chloroform, separation on a 0.8% agarose gel, and visualization with Syber-green.

Acknowledgments

The authors thank Dr M. Michael (Harvard University) for use of the GFP-nucleoplasmin and GFP-hnRNP A1 plasmids and Dr Y. M. Chook (University of Texas Southwestern Medical Center) for the very kind gift of MBP-M3 protein. In addition, we are grateful to Drs Debra Urwin and Jim Kadonaga (UCSD) for the gift of Drosophila core histones and the histone chaperone NAP1. This work was supported in part by a grant from the United States–Israel Binational Science Foundation to M. E. and D. F., by an NIH RO1 grant (GM-R01-33279) to D. F. and by the Gerhard M. J. Schmidt Minerva Center for Supramolecular Architecture at the Weizmann Institute, Israel. This research is made possible in part by and the historic generosity of the Harold Perlman Family.

Supporting Information

Additional Supporting Information may be found in the online version of this article:

Figure S1: Excess GFP-M9 inhibits transportin-mediated, but not importin β-mediated transport. Excess GFP-M9 (40 μM) was added to a *Xenopus* nuclear reconstitution assay 30 min after the start of the reaction. A) TRITC-labeled classical NLS import substrate SV40-NLS-HSA or (B) Alexa-568-labeled transportin substrate MBP-M3 was added 30 min after the addition of the excess GFP-M9. The nuclei were incubated for another 30 min before fixation. Bar: 10 μm.

Figure S2: DNA import in permeabilized HeLa cells is dependent on energy and cytosolic factors. Permeabilized cell assays were performed and analyzed as in Figures 4 and 5, except the transport mixture did not contain (A) an energy regenerating system or (B) a rabbit reticulocyte lysate. GFP-A1 was added at 0.7 μM. GFP is shown in green, DNA staining in blue and CX-Rhodamine-labeled DNA import is shown in red. DNA import images were projected from five z-sections through the middle of the nuclei at 0.5 μm apart using ImageJ software (http://rsb.info.nih.gov/ij/). Bar: 10 μm.

Please note: Wiley-Blackwell are not responsible for the content or functionality of any supporting materials supplied by the authors. Any queries (other than missing material) should be directed to the corresponding author for the article.

References

1. Kasamatsu H, Nakanishi A. How do animal DNA viruses get to the nucleus? Annu Rev Microbiol 1998;52:627–686.
2. Marsh M, Helenius A. Virus entry: open sesame. Cell 2006;124: 729–740.
3. Lechardeur D, Lukacs GL. Nucleocytoplasmic transport of plasmid DNA: a perilous journey from the cytoplasm to the nucleus. Hum Gene Ther 2006;17:882–889.
4. Pouton CW, Wagstaff KM, Roth DM, Moseley GW, Jans DA. Targeted delivery to the nucleus. Adv Drug Deliv Rev 2007;59:698–717.
5. Dowty ME, Williams P, Zhang G, Hagstrom JE, Wolff JA. Plasmid DNA entry into postmitotic nuclei of primary rat myotubes. Proc Natl Acad Sci U S A 1995;92:4572–4576.
6. Hagstrom JE, Ludtke JJ, Bassik MC, Sebestyen MG, Adam SA, Wolff JA. Nuclear import of DNA in digitonin-permeabilized cells. J Cell Sci 1997;110 (Pt 18):2323–2331.
7. Ludtke JJ, Zhang G, Sebestyen MG, Wolff JA. A nuclear localization signal can enhance both the nuclear transport and expression of 1 kb DNA. J Cell Sci 1999;112 (Pt 12):2033–2041.
8. Mesika A, Kiss V, Brumfeld V, Ghosh G, Reich Z. Enhanced intracellular mobility and nuclear accumulation of DNA plasmids associated with a karyophilic protein. Hum Gene Ther 2005;16:200–208.
9. Salman H, Zbaida D, Rabin Y, Chatenay D, Elbaum M. Kinetics and mechanism of DNA uptake into the cell nucleus. Proc Natl Acad Sci U S A 2001;98:7247–7252.
10. Subramanian A, Ranganathan P, Diamond SL. Nuclear targeting peptide scaffolds for lipofection of nondividing mammalian cells. Nat Biotechnol 1999;17:873–877.
11. Zanta MA, Belguise-Valladier P, Behr JP. Gene delivery: a single nuclear localization signal peptide is sufficient to carry DNA to the cell nucleus. Proc Natl Acad Sci U S A 1999;96:91–96.

12. van der Aa MA, Mastrobattista E, Oosting RS, Hennink WE, Koning GA, Crommelin DJ. The nuclear pore complex: the gateway to successful nonviral gene delivery. Pharm Res 2006;23:447–459.
13. Wagstaff KM, Jans DA. Nucleocytoplasmic transport of DNA: enhancing non-viral gene transfer. Biochem J 2007;406:185–202.
14. Shimizu N, Kamezaki F, Shigematsu S. Tracking of microinjected DNA in live cells reveals the intracellular behavior and elimination of extrachromosomal genetic material. Nucleic Acids Res 2005;33:6296–6307.
15. Cohen S, Menut S, Mechali M. Regulated formation of extrachromosomal circular DNA molecules during development in Xenopus laevis. Mol Cell Biol 1999;19:6682–6689.
16. Cohen S, Mechali M. Formation of extrachromosomal circles from telomeric DNA in Xenopus laevis. EMBO Rep 2002;3:1168–1174.
17. Cohen S, Agmon N, Yacobi K, Mislovati M, Segal D. Evidence for rolling circle replication of tandem genes in Drosophila. Nucleic Acids Res 2005;33:4519–26.
18. Abken H, Jungfer H, Albert WH, Willecke K. Immortalization of human lymphocytes by fusion with cytoplasts of transformed mouse L cells. J Cell Biol 1986;103:795–805.
19. Abken H, Butzler C, Willecke K. Immortalization of human lymphocytes by transfection with DNA from mouse L929 cytoplasts. Proc Natl Acad Sci U S A 1988;85:468–472.
20. Abken H, Hegger R, Butzler C, Willecke K. Short DNA sequences from the cytoplasm of mouse tumor cells induce immortalization of human lymphocytes in vitro. Proc Natl Acad Sci U S A 1993;90:6518–6522.
21. Cook A, Bono F, Jinek M, Conti E. Structural biology of nucleocytoplasmic transport. Annu Rev Biochem 2007;76:647–671.
22. Pemberton LF, Paschal BM. Mechanisms of receptor-mediated nuclear import and nuclear export. Traffic 2005;6:187–198.
23. Gorlich D, Kutay U. Transport between the cell nucleus and the cytoplasm. Annu Rev Cell Dev Biol 1999;15:607–660.
24. Strom AC, Weis K. Importin-beta-like nuclear transport receptors. Genome Biol 2001;2:REVIEWS3008.
25. Kau TR, Way JC, Silver PA. Nuclear transport and cancer: from mechanism to intervention. Nat Rev Cancer 2004;4:106–117.
26. Fahrenkrog B, Koser J, Aebi U. The nuclear pore complex: a jack of all trades? Trends Biochem Sci 2004;29:175–182.
27. Peters R. Translocation through the nuclear pore complex: selectivity and speed by reduction-of-dimensionality. Traffic 2005;6:421–427.
28. Lim RY, Aebi U, Fahrenkrog B. Towards reconciling structure and function in the nuclear pore complex. Histochem Cell Biol 2008;129:105–116.
29. Rout MP, Aitchison JD, Suprapto A, Hjertaas K, Zhao Y, Chait BT. The yeast nuclear pore complex: composition, architecture, and transport mechanism. J Cell Biol 2000;148:635–651.
30. Cronshaw JM, Krutchinsky AN, Zhang W, Chait BT, Matunis MJ. Proteomic analysis of the mammalian nuclear pore complex. J Cell Biol 2002;158:915–927.
31. Allen NP, Huang L, Burlingame A, Rexach M. Proteomic analysis of nucleoporin interacting proteins. J Biol Chem 2001;276:29268–29274.
32. Pante N, Aebi U. Toward the molecular dissection of protein import into nuclei. Curr Opin Cell Biol 1996;8:397–406.
33. Stewart M. Molecular mechanism of the nuclear protein import cycle. Nat Rev Mol Cell Biol 2007;8:195–208.
34. Suntharalingam M, Wente SR. Peering through the pore: nuclear pore complex structure, assembly, and function. Dev Cell 2003;4:775–789.
35. Tran EJ, Wente SR. Dynamic nuclear pore complexes: life on the edge. Cell 2006;125:1041–1053.
36. Macara IG. Transport into and out of the nucleus. Microbiol Mol Biol Rev 2001;65:570–594, table of contents.
37. Weis K. Regulating access to the genome: nucleocytoplasmic transport throughout the cell cycle. Cell 2003;112:441–451.
38. Yang W, Gelles J, Musser SM. Imaging of single-molecule translocation through nuclear pore complexes. Proc Natl Acad Sci U S A 2004;101:12887–2892.
39. Macara IG. Why FRET about Ran? Dev Cell 2002;2:379–380.
40. Kopito RB, Elbaum M. Reversibility in nucleocytoplasmic transport. Proc Natl Acad Sci U S A 2007;104:12743–12748.
41. Kopito RB, Elbaum M. Nucleocytoplasmic transport: a thermodynamic mechanism. Hum Front Sci Program J 2009;3:130–141.
42. Gorlich D, Kostka S, Kraft R, Dingwall C, Laskey RA, Hartmann E, Prehn S. Two different subunits of importin cooperate to recognize nuclear localization signals and bind them to the nuclear envelope. Curr Biol 1995;5:383–392.
43. Imamoto N, Shimamoto T, Kose S, Takao T, Tachibana T, Matsubae M, Sekimoto T, Shimonishi Y, Yoneda Y. The nuclear pore-targeting complex binds to nuclear pores after association with a karyophile. FEBS Lett 1995;368:415–419.
44. Radu A, Blobel G, Moore MS. Identification of a protein complex that is required for nuclear protein import and mediates docking of import substrate to distinct nucleoporins. Proc Natl Acad Sci U S A 1995;92:1769–1773.
45. Chi NC, Adam EJ, Adam SA. Sequence and characterization of cytoplasmic nuclear protein import factor p97. J Cell Biol 1995;130:265–274.
46. Lange A, Mills RE, Lange CJ, Stewart M, Devine SE, Corbett AH. Classical nuclear localization signals: definition, function, and interaction with importin alpha. J Biol Chem 2007;282:5101–5105.
47. Conti E, Uy M, Leighton L, Blobel G, Kuriyan J. Crystallographic analysis of the recognition of a nuclear localization signal by the nuclear import factor karyopherin alpha. Cell 1998;94:193–204.
48. Kalderon D, Richardson WD, Markham AF, Smith AE. Sequence requirements for nuclear location of simian virus 40 large-T antigen. Nature 1984;311:33–38.
49. Lanford RE, Butel JS. Construction and characterization of an SV40 mutant defective in nuclear transport of T antigen. Cell 1984;37:801–813.
50. Robbins J, Dilworth SM, Laskey RA, Dingwall C. Two interdependent basic domains in nucleoplasmin nuclear targeting sequence: identification of a class of bipartite nuclear targeting sequence. Cell 1991;64:615–623.
51. Pollard VW, Michael WM, Nakielny S, Siomi MC, Wang F, Dreyfuss G. A novel receptor-mediated nuclear protein import pathway. Cell 1996;86:985–994.
52. Nakielny S, Siomi MC, Siomi H, Michael WM, Pollard V, Dreyfuss G. Transportin: nuclear transport receptor of a novel nuclear protein import pathway. Exp Cell Res 1996;229:261–266.
53. Lee BJ, Cansizoglu AE, Suel KE, Louis TH, Zhang Z, Chook YM. Rules for nuclear localization sequence recognition by karyopherin beta 2. Cell 2006;126:543–558.
54. Mosammaparast N, Guo Y, Shabanowitz J, Hunt DF, Pemberton LF. Pathways mediating the nuclear import of histones H3 and H4 in yeast. J Biol Chem 2002;277:862–868.
55. Muhlhausser P, Muller EC, Otto A, Kutay U. Multiple pathways contribute to nuclear import of core histones. EMBO Rep 2001;2:690–696.
56. Baake M, Bauerle M, Doenecke D, Albig W. Core histones and linker histones are imported into the nucleus by different pathways. Eur J Cell Biol 2001;80:669–677.
57. Adam SA, Marr RS, Gerace L. Nuclear protein import in permeabilized mammalian cells requires soluble cytoplasmic factors. J Cell Biol 1990;111:807–816.
58. Newmeyer DD, Finlay DR, Forbes DJ. In vitro transport of a fluorescent nuclear protein and exclusion of non-nuclear proteins. J Cell Biol 1986;103:2091–2102.
59. Newmeyer DD, Wilson KL. Egg extracts for nuclear import and nuclear assembly reactions. Methods Cell Biol 1991;36:607–634.
60. Newport J. Nuclear reconstitution in vitro: stages of assembly around protein-free DNA. Cell 1987;48:205–217.
61. Smythe C, Newport JW. Systems for the study of nuclear assembly, DNA replication, and nuclear breakdown in Xenopus laevis egg extracts. Methods Cell Biol 1991;35:449–468.
62. Smith DE, Tans SJ, Smith SB, Grimes S, Anderson DL, Bustamante C. The bacteriophage straight phi29 portal motor can package DNA against a large internal force. Nature 2001;413:748–752.
63. Maier B, Chen I, Dubnau D, Sheetz MP. DNA transport into Bacillus subtilis requires proton motive force to generate large molecular forces. Nat Struct Mol Biol 2004;11:643–649.
64. Allen NP, Patel SS, Huang L, Chalkley RJ, Burlingame A, Lutzmann M, Hurt EC, Rexach M. Deciphering networks of protein interactions at the nuclear pore complex. Mol Cell Proteomics 2002;1:930–946.

65. Snay-Hodge CA, Colot HV, Goldstein AL, Cole CN. Dbp5p/Rat8p is a yeast nuclear pore-associated DEAD-box protein essential for RNA export. Embo J 1998;17:2663–2676.
66. Tseng SS, Weaver PL, Liu Y, Hitomi M, Tartakoff AM, Chang TH. Dbp5p, a cytosolic RNA helicase, is required for poly(A)+ RNA export. Embo J 1998;17:2651–2662.
67. Finlay DR, Forbes DJ. Reconstitution of biochemically altered nuclear pores: transport can be eliminated and restored. Cell 1990;60:17–29.
68. Newmeyer DD, Forbes DJ. Nuclear import can be separated into distinct steps in vitro: nuclear pore binding and translocation. Cell 1988;52:641–653.
69. Walther TC, Pickersgill HS, Cordes VC, Goldberg MW, Allen TD, Mattaj IW, Fornerod M. The cytoplasmic filaments of the nuclear pore complex are dispensable for selective nuclear protein import. J Cell Biol 2002;158:63–77.
70. Drummond SP, Wilson KL. Interference with the cytoplasmic tail of gp210 disrupts ''close apposition'' of nuclear membranes and blocks nuclear pore dilation. J Cell Biol 2002;158:53–62.
71. Gant TM, Goldberg MW, Allen TD. Nuclear envelope and nuclear pore assembly: analysis of assembly intermediates by electron microscopy. Curr Opin Cell Biol 1998;10:409–415.
72. Goldberg MW, Wiese C, Allen TD, Wilson KL. Dimples, pores, star-rings, and thin rings on growing nuclear envelopes: evidence for structural intermediates in nuclear pore complex assembly. J Cell Sci 1997;110 (Pt 4):409–420.
73. Harel A, Chan RC, Lachish-Zalait A, Zimmerman E, Elbaum M, Forbes DJ. Importin beta negatively regulates nuclear membrane fusion and nuclear pore complex assembly. Mol Biol Cell 2003;14:4387–4396.
74. Harel A, Orjalo AV, Vincent T, Lachish-Zalait A, Vasu S, Shah S, Zimmerman E, Elbaum M, Forbes DJ. Removal of a single pore subcomplex results in vertebrate nuclei devoid of nuclear pores. Mol Cell 2003;11:853–864.
75. Macaulay C, Forbes DJ. Assembly of the nuclear pore: biochemically distinct steps revealed with NEM, GTP gamma S, and BAPTA. J Cell Biol 1996;132:5–20.
76. Zhang C, Goldberg MW, Moore WJ, Allen TD, Clarke PR. Concentration of Ran on chromatin induces decondensation, nuclear envelope formation and nuclear pore complex assembly. Eur J Cell Biol 2002;81:623–633.
77. Heald R, Tournebize R, Habermann A, Karsenti E, Hyman A. Spindle assembly in Xenopus egg extracts: respective roles of centrosomes and microtubule self-organization. J Cell Biol 1997;138:615–628.
78. Zhang C, Hughes M, Clarke PR. Ran-GTP stabilises microtubule asters and inhibits nuclear assembly in Xenopus egg extracts. J Cell Sci 1999;112 (Pt 14):2453–2461.
79. Kalab P, Pu RT, Dasso M. The ran GTPase regulates mitotic spindle assembly. Curr Biol 1999;9:481–484.
80. Orjalo AV, Arnaoutov A, Shen Z, Boyarchuk Y, Zeitlin SG, Fontoura B, Briggs S, Dasso M, Forbes DJ. The Nup107-160 nucleoporin complex is required for correct bipolar spindle assembly. Mol Biol Cell 2006;17:3806–3818.
81. Pruschy M, Ju Y, Spitz L, Carafoli E, Goldfarb DS. Facilitated nuclear transport of calmodulin in tissue culture cells. J Cell Biol 1994;127:1527–1536.
82. Yoneda Y, Imamoto-Sonobe N, Yamaizumi M, Uchida T. Reversible inhibition of protein import into the nucleus by wheat germ agglutinin injected into cultured cells. Exp Cell Res 1987;173:586–595.
83. Dabauvalle MC, Schulz B, Scheer U, Peters R. Inhibition of nuclear accumulation of karyophilic proteins in living cells by microinjection of the lectin wheat germ agglutinin. Exp Cell Res 1988;174:291–296.
84. Schulz B, Peters R. Nucleocytoplasmic protein traffic in single mammalian cells studied by fluorescence microphotolysis. Biochim Biophys Acta 1987;930:419–431.
85. Finlay DR, Newmeyer DD, Price TM, Forbes DJ. Inhibition of in vitro nuclear transport by a lectin that binds to nuclear pores. J Cell Biol 1987;104:189–200.
86. Kutay U, Izaurralde E, Bischoff FR, Mattaj IW, Gorlich D. Dominant-negative mutants of importin-beta block multiple pathways of import and export through the nuclear pore complex. Embo J 1997;16:1153–1163.
87. Jaggi RD, Franco-Obregon A, Muhlhausser P, Thomas F, Kutay U, Ensslin K. Modulation of nuclear pore topology by transport modifiers. Biophys J 2003;84:665–670.
88. Hughes M, Zhang C, Avis JM, Hutchison CJ, Clarke PR. The role of the ran GTPase in nuclear assembly and DNA replication: characterisation of the effects of Ran mutants. J Cell Sci 1998;111 (Pt 20):3017–3026.
89. Nakielny S, Shaikh S, Burke B, Dreyfuss G. Nup153 is an M9-containing mobile nucleoporin with a novel Ran-binding domain. Embo J 1999;18:1982–1995.
90. Shah S, Tugendreich S, Forbes D. Major binding sites for the nuclear import receptor are the internal nucleoporin Nup153 and the adjacent nuclear filament protein Tpr. J Cell Biol 1998;141:31–49.
91. Ullman KS, Shah S, Powers MA, Forbes DJ. The nucleoporin nup153 plays a critical role in multiple types of nuclear export. Mol Biol Cell 1999;10:649–664.
92. Walther TC, Fornerod M, Pickersgill H, Goldberg M, Allen TD, Mattaj IW. The nucleoporin Nup153 is required for nuclear pore basket formation, nuclear pore complex anchoring and import of a subset of nuclear proteins. Embo J 2001;20:5703–5714.
93. Shah S, Forbes DJ. Separate nuclear import pathways converge on the nucleoporin Nup153 and can be dissected with dominant-negative inhibitors. Curr Biol 1998;8:1376–1386.
94. Blow JJ, Laskey RA. Initiation of DNA replication in nuclei and purified DNA by a cell-free extract of Xenopus eggs. Cell 1986;47:577–587.
95. Wilson GL, Dean BS, Wang G, Dean DA. Nuclear import of plasmid DNA in digitonin-permeabilized cells requires both cytoplasmic factors and specific DNA sequences. J Biol Chem 1999;274:22025–22032.
96. Saphire AC, Guan T, Schirmer EC, Nemerow GR, Gerace L. Nuclear import of adenovirus DNA in vitro involves the nuclear protein import pathway and hsc70. J Biol Chem 2000;275:4298–4304.
97. Moroianu J, Blobel G. Protein export from the nucleus requires the GTPase Ran and GTP hydrolysis. Proc Natl Acad Sci U S A 1995;92:4318–4322.
98. Holaska JM, Paschal BM. A cytosolic activity distinct from crm1 mediates nuclear export of protein kinase inhibitor in permeabilized cells. Proc Natl Acad Sci U S A 1998;95:14739–14744.
99. Rosenblum JS, Pemberton LF, Bonifaci N, Blobel G. Nuclear import and the evolution of a multifunctional RNA-binding protein. J Cell Biol 1998;143:887–899.
100. Chook YM, Jung A, Rosen MK, Blobel G. Uncoupling Kap-beta2 substrate dissociation and ran binding. Biochemistry 2002;41:6955–6966.
101. Bayliss R, Leung SW, Baker RP, Quimby BB, Corbett AH, Stewart M. Structural basis for the interaction between NTF2 and nucleoporin FxFG repeats. Embo J 2002;21:2843–2853.
102. Lukacs GL, Haggie P, Seksek O, Lechardeur D, Freedman N, Verkman AS. Size-dependent DNA mobility in cytoplasm and nucleus. J Biol Chem 2000;275:1625–1629.
103. Mosammaparast N, Jackson KR, Guo Y, Brame CJ, Shabanowitz J, Hunt DF, Pemberton LF. Nuclear import of histone H2A and H2B is mediated by a network of karyopherins. J Cell Biol 2001;153:251–262.
104. Baake M, Doenecke D, Albig W. Characterisation of nuclear localisation signals of the four human core histones. J Cell Biochem 2001;81:333–346.
105. Ito T, Bulger M, Kobayashi R, Kadonaga JT. Drosophila NAP-1 is a core histone chaperone that functions in ATP-facilitated assembly of regularly spaced nucleosomal arrays. Mol Cell Biol 1996;16:3112–3124.
106. Trotman LC, Mosberger N, Fornerod M, Stidwill RP, Greber UF. Import of adenovirus DNA involves the nuclear pore complex receptor CAN/Nup214 and histone H1. Nat Cell Biol 2001;3:1092–1100.
107. Hindley CE, Lawrence FJ, Matthews DA. A role for transportin in the nuclear import of adenovirus core proteins and DNA. Traffic 2007;8:1313–1322.
108. Herweijer H, Wolff JA. Progress and prospects: naked DNA gene transfer and therapy. Gene Ther 2003;10:453–458.
109. Luby-Phelps K. Cytoarchitecture and physical properties of cytoplasm: volume, viscosity, diffusion, intracellular surface area. Int Rev Cytol 2000;192:189–221.
110. Suel KE, Gu H, Chook YM. Modular organization and combinatorial energetics of proline-tyrosine nuclear localization signals. PLoS Biol 2008;6:e137.

111. Mosammaparast N, Pemberton LF. Karyopherins: from nuclear-transport mediators to nuclear-function regulators. Trends Cell Biol 2004;14:547–556.
112. Pinol-Roma S, Dreyfuss G. Shuttling of pre-mRNA binding proteins between nucleus and cytoplasm. Nature 1992;355:730–732.
113. Johnson-Saliba M, Siddon NA, Clarkson MJ, Tremethick DJ, Jans DA. Distinct importin recognition properties of histones and chromatin assembly factors. FEBS Lett 2000;467:169–174.
114. Marcello M, Fischer R, Troster H, Trendelenburg MF, Sczakiel G. Selecting karyophilic DNA cis elements in Xenopus laevis oocytes; a new approach. Int J Dev Biol 2002;46:309–316.
115. Mosammaparast N, Del Rosario BC, Pemberton LF. Modulation of histone deposition by the karyopherin kap114. Mol Cell Biol 2005;25:1764–1778.
116. Laigle A, Chinsky L, Turpin PY, Liquier J, Taillandier E. In vitro recognition of DNA base pairs by histones in histone-DNA complexes and reconstituted core particles: an ultraviolet resonance Raman study. Nucleic Acids Res 1982;10:7395–404.
117. Kuttler F, Mai S. Formation of non-random extrachromosomal elements during development, differentiation and oncogenesis. Semin Cancer Biol 2007;17:56–64.
118. Shcheprova Z, Baldi S, Frei SB, Gonnet G, Barral Y. A mechanism for asymmetric segregation of age during yeast budding. Nature 2008;454:728–734.
119. Schoenlein PV, Shen DW, Barrett JT, Pastan I, Gottesman MM. Double minute chromosomes carrying the human multidrug resistance 1 and 2 genes are generated from the dimerization of submicroscopic circular DNAs in colchicine-selected KB carcinoma cells. Mol Biol Cell 1992;3:507–520.
120. Vogt N, Lefèvre SH, Apiou F, Dutrillaux AM, Cör A, Leuraud P, Poupon MF, Dutrillaux B, Debatisse M, Malfoy B. Molecular structure of double-minute chromosomes bearing amplified copies of the epidermal growth factor receptor gene in gliomas. Proc Natl Acad Sci U S A 2004;101:11368–11373.
121. Von Hoff DD, Forseth B, Clare CN, Hansen KL, VanDevanter D. Double minutes arise from circular extrachromosomal DNA intermediates which integrate into chromosomal sites in human HL-60 leukemia cells. J Clin Invest 1990;85:1887–1895.
122. Cohen S, Regev A, Lavi S. Small polydispersed circular DNA (spcDNA) in human cells: association with genomic instability. Oncogene 1997;14:977–985.
123. Nakazono M, Hirai A. Frequent DNA transfer among mitochondrial, plastid and nuclear genomes of rice during evolution. In: Hirano HY, Sano Y, Hirai A, Sasaki T, editors. Biotechnology in Agriculture and Forestry, Volume 62. New York: Springer Berlin Heidelberg; 2008, pp. 107–117.
124. Kim JH, Antunes A, Luo SJ, Menninger J, Nash WG, O'Brien SJ, Johnson WE. Evolutionary analysis of a large mtDNA translocation (numt) into the nuclear genome of the Panthera genus species. Gene 2006;366:292–302.
125. Martin W, Rujan T, Richly E, Hansen A, Cornelsen S, Lins T, Leister D, Stoebe B, Hasegawa M, Penny D. Evolutionary analysis of Arabidopsis, cyanobacterial, and chloroplast genomes reveals plastid phylogeny and thousands of cyanobacterial genes in the nucleus. Proc Natl Acad Sci U S A 2002;99:12246–12251.
126. Chan RC, Forbes DJ. In vitro study of nuclear assembly and nuclear import using Xenopus egg extracts. Methods Mol Biol 2006;322:289–300.
127. Allen TD, Rutherford SA, Bennion GR, Wiese C, Riepert S, Kiseleva E, Goldberg MW. Three-dimensional surface structure analysis of the nucleus. Methods Cell Biol 1998;53:125–138.